Journal of Magnetic Resonance 199 (2009) 192–198

Contents lists available at ScienceDirect

Journal of Magnetic Resonance

journal homepage: www.elsevier.com/locate/jmr

Experimental access to HSQC spectra decoupled in all frequency dimensions

Peyman Sakhaii [a,1], Burkhard Haase [a,1], Wolfgang Bermel [b,*]

[a] Sanofi-Aventis Deutschland GmbH, Process Development Chemistry, PDC SPS (Structure Elucidation/Project & Production Support), Industriepark Hoechst, Building G838, Labor 204, D-65926 Frankfurt/Main, Germany
[b] Bruker BioSpin GmbH, Silberstreifen, D-76287 Rheinstetten, Germany

ARTICLE INFO

Article history:
Received 4 February 2009
Revised 20 April 2009
Available online 6 May 2009

This work is dedicated to electrical engineer Hassan Sakhaii who passed away on July 27th 2008

Keywords:
Homodecoupling
Pure shift spectra
SHARC
Constant time acquisition
Frequency dependent folding

ABSTRACT

A new operator called RESET "Reducing nuclEar Spin multiplicitiEs to singuleTs" is presented to acquire broadband proton decoupled proton spectra in one and two dimensions. Basically, the homonuclear decoupling is achieved through the application of bilinear rotation pulses and delays. A $[BIRD]^{r,x}$ pulse building block is used to selectively invert all proton magnetization remotely attached to ^{13}C isotopes, which is equivalent to a scalar J decoupling of the protons directly attached to ^{13}C from all other protons in the spin system. In conjunction with an appropriate data processing technique pure shift proton spectra are obtained. For this purpose, the concept of constant time acquisition in the observe dimension is exploited. Both ideas were merged together producing superior HSQC based pseudo 3D pulse sequences. The resulting HSQC spectra show cross peaks with collapsed multiplet structures and singlet responses for the proton chemical shift frequencies. An unambiguous assignment of signals from overcrowded spectra becomes much easier. Finally, the recently introduced SHARC technique is exploited to enhance the capability of the scalar J decoupling method. A significant reduction of the total measurement time is achieved. The time is saved by reducing the number of ^{13}C chemical shift evolution increments and working with superimposed narrow spectral bandwidths in the ^{13}C indirect domain.

© 2009 Elsevier Inc. All rights reserved.

1. Introduction

Since the very early days of NMR there has been a growing interest in developing spectroscopic techniques to remove the effect of scalar *J* coupling from the NMR spectra of coupled spin pairs [1]. Therefore the area of homo and heteronuclear decoupling techniques became an exciting field for the development of useful NMR pulse sequences [2,3].

A variety of different techniques were introduced to obtain broadband homonuclear decoupled proton spectra, which have to be classified in two different groups. The first group achieves the elimination of scalar J coupling by selective RF irradiation in the *observe dimension* using stroboscopic data point acquisition. The second group performs the homonuclear decoupling in the *indirect dimension* or is exploiting the data acquired in the indirect dimension for reconstruction of the one dimensional scalar *J* decoupled spectrum. One of the difficulties for the creation of a homonuclear decoupling sequence is the necessity for the selective inversion of one of the spins. As this usually means inversion of a small bandwidth, this would lead to applying shaped RF pulses of unacceptable length.

Conventional homodecoupling is performed by decoupling a single ^1H multiplet [4]. The final decoupled spectrum displays conventional ^1H resonance lines but all scalar *J* couplings arising from this decoupled spin have been removed. Thus, multiplets are simplified and coupling constants and signal patterns can be extracted. Practically, a selective RF irradiation is applied at a resonance frequency during the acquisition time. This RF irradiation takes place during a given fraction of the nominal dwell time (hdduty). During this time the receiver is gated off, which reduces the overall sensitivity. The extension of homodecoupling is the band-selective homodecoupling [5–7]. In analogy to CW decoupling, a shaped inversion RF pulse is applied during the data acquisition. The execution of the shaped inversion RF pulse is interrupted by the stroboscopic data point acquisition. This leads to an amplitude modulated DANTE type [8] decoupling pulse. With this approach it is not possible to achieve broadband homonuclear decoupling.

Different approaches were suggested for this purpose. A first example is the so-called *J* resolved spectroscopy. The experiment is based on a spin echo sequence and shows pure *J* evolution in the indirect (F_1) and *J* as well as chemical shift evolution in the observe (F_2) dimension. Hence the resulting spectrum shows tilted multiplets, whereby the tilt angle depends on the ratio of the dwell times in the two dimensions. Shearing the spectrum

* Corresponding author. Fax: +49 0 721 5161 297.
E-mail addresses: Peyman.Sakhaii@sanofi-aventis.com (P. Sakhaii), Burkhard.Haase@sanofi-aventis.com (B. Haase), Wolfgang.Bermel@bruker-biospin.de (W. Bermel).
[1] Fax: +49 0 69 305 24766.

1090-7807/$ - see front matter © 2009 Elsevier Inc. All rights reserved.
doi:10.1016/j.jmr.2009.04.016

results in a separation of J information in the F_1 and chemical shift in the F_2 dimension. A projection onto the F_2 axis finally yields a broadband decoupled proton spectrum. Unfortunately, the J resolved spectrum has a phase-twisted lineshape and hence the data has to be processed in magnitude mode [9]. Extensive backward linear prediction has been suggested to remove the twisted lineshape [10].

Alternative methods are based on the symmetry properties of multiplets. One produces 2D spectra in which the multiplets have structures with rotational symmetry pattern (C_{4v} symmetry). This property is exploited in a software program that locates the symmetry centers of the two dimensional multiplets. These symmetry centers are taken as a measure of the chemical shifts for the construction of the decoupled spectrum [11]. Another selects certain lines of a multiplet [12].

Another approach to obtain pure shift spectra was reported based on a 45° projection of the diagonal peak of an anti z-COSY [13]. The proposed method delivers decoupled spectra that have absorption mode lineshapes and retain the correct integrals. Unfortunately, there are a number of drawbacks associated with this method. It requires the acquisition of a large number of data points along the ω_1 time axis to ensure that the line width is determined by relaxation and not by insufficient sampling. A considerable reduction in sensitivity must be taken into account compared to a regular proton spectrum, due to the use of two small flip angle pulses (10°). Another problem is the presence of strong coupling, which leads to additional peaks in the homodecoupled spectrum. A feature, which can be found in two dimensional J spectra as well.

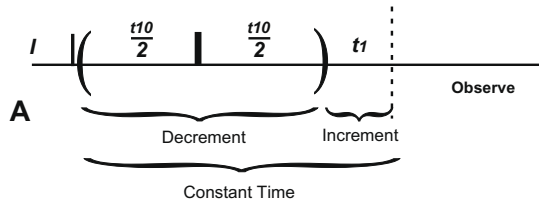

Fig. 1. A simple constant time spin echo pulse sequence is displayed. A constant time delay of 126 ms was used. The incrementation delay was set to the length of a complex dwell time in the observe dimension.

Earlier, a simple scheme for in-phase selective excitation of overlapping multiplets was proposed [14–16]. The chemical shift filtration CSSF was achieved by a combination of a train of selective and non-selective 180° pulses. The magnetization within the inversion bandwidth of the 180° selective pulse experiences a 360° pulse, while the magnetization outside of this region is inverted by the non-selective 180° pulse. This corresponds to a refocusing of the homonuclear J coupling for those spins being inside the inversion bandwidth of the 180° selective pulse [17,18]. So a homonuclear J decoupling is only achievable for a fraction of entire frequency bandwidth per unit time. Decoupling the full proton chemical shift range would require to move the CSSF filter over the whole chemical shift bandwidth and repeat the acquisition for those regions.

Zangger and Sterk have found a very elegant way to sidestep this difficulty by creating a spatial selective CSSF filter [19]. Here, the combination of the selective and non-selective 180° proton pulses in the presence of a weak rectangular z gradient pulse forms a spatial selective homonuclear J decoupling scheme. The entire chemical shift becomes spatial dependent along the main axis of the weak gradient pulse. The whole volume of the sample must be thought of as being divided into slices. Each slice gives rise to signals from a different spectral region, hence eliminating the need to shift the filter. A new FID is reconstructed from data acquired as a pseudo 2D experiment. Conceptionally this is the first column of the two dimensional data. In order to reduce the experiment time, the number of increments is reduced and blocks of data along the acquisition dimension are used for reconstruction. These data blocks are typically 8 ms in length. While recording the data points in t_2 homonuclear J modulation occurs, leading to sidebands in the final spectrum. The amount

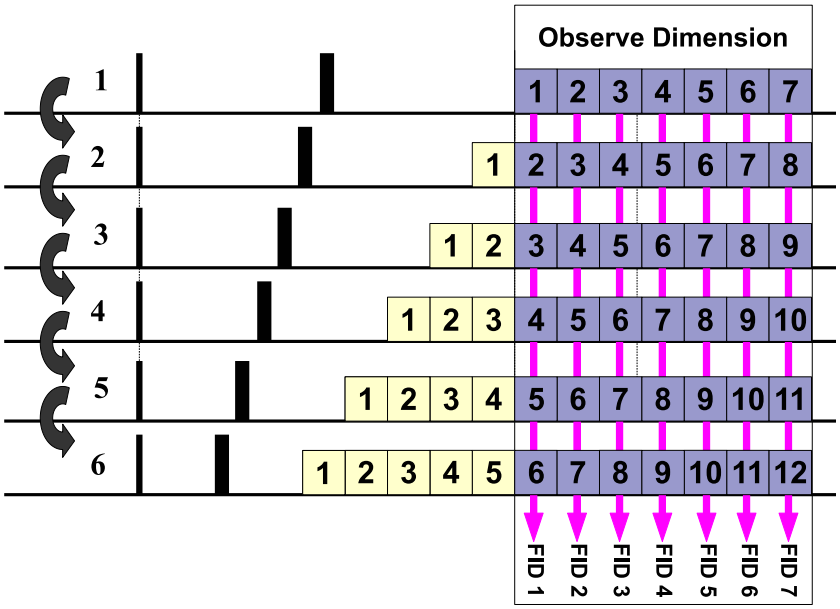

Fig. 2. This figure displays, how pulse program A was used to acquire the constant time data matrix of chemical shift evolution. Each rectangular box corresponds to a complex dwell point in the observe dimension. The incrementation delay of the indirect dimension was set to the length of a complex dwell time in the observe dimension t_2. The arrows are indicating the subsequent progress of the experiment in ω_1. Actual data acquisition is indicated by a box. New FIDs along the pseudo ω_1 dimension were reconstructed by taking the columns at constant time points followed by right shift and back prediction procedures according to the number of missing complex dwell points. The final FID is computed by simply adding up the individual FIDs. Basically, the right shift and back prediction operations are important steps enabling a coherent phase evolution of each single FID without a large base line distortion.

of sidebands being acceptable defines the upper limit of the block length. The selective 180° refocusing pulse employed for the spatial frequency selection implicates that only a fraction of the sample volume contributes to a given chemical shift in the final spectrum. The performance of *J* decoupling strongly depends on the length of the selective inversion pulses. An unlimited increase of the length of the shaped pulses will lead to significant loss of signal intensity induced by diffusion phenomena [20]. A considerable reduction of signal-to-noise must be accepted. About 2% of the original signal intensity are expected to be retained [20,21].

Very recently, Gareth Morris introduced an improved version of the original Zangger-Sterk method to remove homonuclear spin–spin splitting in DOSY spectra [22]. The spatial selective 180° pulses were phase cycled and accompanied by bipolar gradient pulses for a clean and better selection of the desired coherence transfer pathway.

For heteronuclear correlation experiments on molecules, where the heteronuclear spins are in natural abundance, a combination with the Zangger-Sterk method is feasible, but the overall sensitivity is going to be quite low. We present here a new approach, which is based on isotope rather than spatial selection. In addition a modified data processing scheme further enhances the sensitivity.

2. Results and discussions

The modification of the data processing scheme is best illustrated when looking at an experiment with constant time (CT) acquisition. This provides an easy way to obtain pure shift spectra in ω_1. The concept of the constant time acquisition has been used for a long time for example in Bio-NMR spectroscopy of fully ^{13}C isotope labelled proteins. It results in spectra with removed spin–spin *J* splitting [23,24]. The mechanism behind such a concept is mainly to keep the evolution of the homonuclear *J* coupling constant, while at the same time the evolution of the chemical shift is maintained. Fourier Transformation of such a data set delivers collapsed multiplet structures. The pure shift spectra were mainly reconstructed from ω_1 projections. This requires the *J* coupling to be uniform throughout the molecule. Otherwise the *J* evolution during the constant time will modulate the intensity of the singlet responses in the pure shift spectrum.

The experiment for obtaining pure shift spectra in one and two dimensions is based on pulse sequence A (Fig. 1). In this pulse sequence, a chosen time period is kept constant by synchronizing the t_1 and t_{10} evolution increments. The CT pulse sequence A generates the data matrix displayed in Fig. 2. In contrast to the original paper [24] we process the pseudo 2D data points differently. For a better understanding of our processing strategy, the time evolution of proton chemical shift is indicated by labelling the associated dwell points with a running integer number (Fig. 2). The increments for t_1 and t_{10} (in1 and in10) in the indirect dimension were set to the length of a dwell time (dw) between complex points in the observe dimension t_2, thus synchronizing the two. As indicated in Fig. 2, a single column corresponds to a FID of a CT type spectrum. No spin–spin *J* splitting is observed in its spectrum after FT of this FID, since except for chemical shift, the evolution of relaxation and *J* coupling along the ω_1 time axis is kept constant.

The first column represents a pure shift spectrum, since it contains all required dwell points starting from 1 to 6 (Fig. 2). As it turns out the second column represents a pure shift spectrum as well, but with the first dwell point now missing. Along the same line, there is a gap of dwell points at the beginning of the following columns, with the number of missing points increasing. As long as the chemical shift evolution of the different columns is synchronized with the observe dwell time, the missing data points can be back predicted. The data reconstruction is achieved by first right shifting the data points by the required number and then back predicting the missing dwell points of the individual columns. Finally summation of all individual reconstructed FIDs will yield the final FID. This final FID displays a pure shift spectrum with absorption mode line shape. It is clear that there is a limitation for the back prediction of missing data points. This limitation implies a maximum number of columns, which can be included in the reconstruction procedure. In our hand we have included columns from a maximum t_2 evolution time of 20 ms. Through the cumulative addition of each single reconstructed FID the intensity of the final signal is increased. The signal intensities from random noise are increasing more slowly (square root) while co-adding the data points. Overall signal amplitudes are still weighted by the *J* coupling and relaxation.

A thorough analysis of our data processing strategy is exemplified on the basis of the Eq. (1), the 2D data point matrix, which forms the output of the pulse sequence A (Fig. 1). The description includes a treatment of relaxation and spin–spin *J* coupling.

$$\begin{bmatrix} \Omega_1 R_1 J_1 & \Omega_2 R_2 J_2 & \Omega_3 R_3 J_3 & \cdots & \Omega_n R_n J_n \\ \Omega_2 R_1 J_1 & \Omega_3 R_2 J_2 & \Omega_4 R_3 J_3 & \cdots & \Omega_{(n+1)} R_n J_n \\ \Omega_3 R_1 J_1 & \Omega_4 R_2 J_2 & \Omega_5 R_3 J_3 & \cdots & \Omega_{(n+2)} R_n J_n \\ \vdots & \vdots & \vdots & & \vdots \\ \Omega_n R_1 J_1 & \Omega_{(n+1)} R_2 J_2 & \Omega_{(n+2)} R_3 J_3 & \cdots & \Omega_{(2n-1)} R_n J_n \end{bmatrix} = \begin{bmatrix} \mathrm{FID}_1^0 \\ \mathrm{FID}_2^0 \\ \mathrm{FID}_3^0 \\ \vdots \\ \mathrm{FID}_n^0 \end{bmatrix} \quad (1)$$

Each row of the matrix corresponds to the FID of the constant time pseudo 2D experiment. For one spin (I_{1x}) of a two spin system the evolution of chemical shift (Ω), *J* coupling (J_{12}) and relaxation (R) during the acquisition time (t) can be described by:

$$[I_{1x}\cos(\pi J_{12}t) + 2I_{1y}I_{2z}\sin(\pi J_{12}t)] \times \exp(-iQt) \times \exp(-Rt)$$

Each cell of the matrix is representing a complex dwell point, where Ω_i, J_i and R_i symbolize the amount of evolution of chemical shift, spin–spin *J* coupling and relaxation at a given time point t_i (a zero in the matrix indicates a point where no data is available). Now, the next step is to transpose the matrix of Eq. (1) to derive the new matrix of Eq. (2)

$$\begin{bmatrix} \Omega_1 R_1 J_1 & \Omega_2 R_1 J_1 & \Omega_3 R_1 J_1 & \cdots & \Omega_n R_1 J_1 \\ \Omega_2 R_2 J_2 & \Omega_3 R_2 J_2 & \Omega_4 R_2 J_2 & \cdots & \Omega_{(n+1)} R_2 J_2 \\ \Omega_3 R_3 J_3 & \Omega_4 R_3 J_3 & \Omega_5 R_3 J_3 & \cdots & \Omega_{(n+2)} R_3 J_3 \\ \vdots & \vdots & \vdots & & \vdots \\ \Omega_n R_n J_n & \Omega_{(n+1)} R_n J_n & \Omega_{(n+2)} R_n J_n & \cdots & \Omega_{(2n-1)} R_n J_n \end{bmatrix} = \begin{bmatrix} \mathrm{FID}_1 \\ \mathrm{FID}_2 \\ \mathrm{FID}_3 \\ \vdots \\ \mathrm{FID}_n \end{bmatrix} \quad (2)$$

A set of new FIDs has been created based on the dwell points of each individual row. Essentially, for each new FID, the evolution of relaxation and *J* coupling is kept constant. Consequently, each row describes a pure shift spectrum after FT. Those signal intensities are weighted by the contribution of spin–spin *J* coupling and relaxation (Eq. (2)). The next processing step includes a right shift operation on the data points of each single row by the number of missing dwell points to produce the matrix of Eq. (3). This is an important step in order to synchronize the evolution of the chemical shifts in the different rows.

$$\begin{bmatrix} \Omega_1R_1J_1 & \Omega_2R_1J_1 & \Omega_3R_1J_1 & \cdots & \cdots & \cdots & \Omega_nR_1J_1 & 0 & 0 & 0 & 0 \\ 0 & \Omega_2R_2J_2 & \Omega_3R_2J_2 & \Omega_4R_2J_2 & \cdots & \cdots & \cdots & \Omega_{(n+1)}R_2J_2 & 0 & 0 & 0 \\ 0 & 0 & \Omega_3R_3J_3 & \Omega_4R_3J_3 & \Omega_5R_3J_3 & \cdots & \cdots & \cdots & \Omega_{(n+2)}R_3J_3 & 0 & 0 \\ \vdots & \vdots & \vdots & \vdots & \vdots & \vdots & \vdots & \vdots & \vdots & \vdots & \vdots \\ 0 & 0 & 0 & 0 & 0 & \cdots & \Omega_nR_nJ_n & \Omega_{(n+1)}R_nJ_n & \Omega_{(n+2)}R_nJ_n & \cdots & \Omega_{(2n-1)}R_nJ_n \end{bmatrix} = \begin{bmatrix} \mathrm{FID}_1 \\ \mathrm{FID}_2 \\ \mathrm{FID}_3 \\ \vdots \\ \mathrm{FID}_n \end{bmatrix} \quad (3)$$

A back prediction procedure has to be applied on each single FID described by Eq. (3). A regular back prediction algorithm is used to replace the zeros with calculated data points leading to Eq. (4). This step is included into our processing scheme to avoid large first order phase correction of each single FID after FT. The back calculation procedures ensure a coherent phase and baseline correction of all reconstructed FIDs after FT. The numerical result is given in Eq. (4).

$$\begin{bmatrix} \Omega_1R_1J_1 & \Omega_2R_1J_1 & \Omega_3R_1J_1 & \cdots & \cdots & \cdots & \Omega_nR_1J_1 & 0 & 0 & 0 & 0 \\ [\boldsymbol{\Omega_1R_2J_2}] & \Omega_2R_2J_2 & \Omega_3R_2J_2 & \Omega_4R_2J_2 & \cdots & \cdots & \cdots & \Omega_{(n+1)}R_2J_2 & 0 & 0 & 0 \\ [\boldsymbol{\Omega_1R_3J_3}] & [\boldsymbol{\Omega_2R_3J_3}] & \Omega_3R_3J_3 & \Omega_4R_3J_3 & \Omega_5R_3J_3 & \cdots & \cdots & \cdots & \Omega_{(n+2)}R_3J_3 & 0 & 0 \\ \vdots & \vdots & \vdots & \vdots & \vdots & \vdots & \vdots & \vdots & \vdots & \vdots & \vdots \\ [\boldsymbol{\Omega_1R_nJ_n}] & [\boldsymbol{\Omega_2R_nJ_n}] & [\boldsymbol{\Omega_3R_nJ_n}] & [\boldsymbol{\Omega_4R_nJ_n}] & [\boldsymbol{\Omega_5R_nJ_n}] & \cdots & \Omega_nR_nJ_n & \Omega_{(n+1)}R_nJ_n & \Omega_{(n+2)}R_nJ_n & \cdots & \Omega_{(2n-1)}R_nJ_n \end{bmatrix} = \begin{bmatrix} \mathrm{FID}_1 \\ \mathrm{FID}_2 \\ \mathrm{FID}_3 \\ \vdots \\ \mathrm{FID}_n \end{bmatrix} \quad (4)$$

The final FID is computed by summation of individual FIDs.

$$\mathbf{FID}_1 + \mathbf{FID}_2 + \mathbf{FID}_3 + \ldots + \mathbf{FID}_n + = \mathbf{FID}_{\mathrm{final}} \quad (5)$$

The final FID provides a pretty spectrum after FT with removed spin–spin J splitting at the chemical shift frequencies. However, all signal intensities are severely affected by the effect of J coupling and relaxation, both evolving during the constant time period.

Fig. 3B shows the experimental proof of our processing technique and demonstrates a simple 1D pure shift proton spectrum of Quinine. The spectrum was recorded by utilizing pulse sequence A (Fig. 1) and treating the acquired pseudo 2D data point matrix as described above. The spectrum has an absorption mode line shape and gives singlet response for the chemical shift frequencies. As indicated earlier, the corresponding peak intensities are weighted by the evolution of J coupling and relaxation.

Obviously there is a strong necessity to remove those adverse properties to improve the spectrum quality. Therefore, we have optimized our data acquisition scheme by eliminating the effect of homonuclear spin–spin J coupling in the preparation period. This requires the application of a J decoupling block in the middle of the constant time period. For this we used a J selective BIRD filter. The cluster of bilinear rotation pulses and delays is widely used in heteronuclear NMR experiments for J selective spin inversion [25–28]. Various BIRD pulses have been published, which differ in the relative phase and number of their individual pulses. They have been mainly used in evolution or mixing periods to selectively invert proton spins attached to ^{13}C isotopes, while leaving those attached to ^{12}C unaffected. This is possible, because in such a heteronuclear spin system the $^1J_{HC}$ couplings are substantially larger than the $^nJ_{HC}$ long-range couplings and all proton–proton couplings.

Here we use a different type of BIRD pulse, a $[BIRD]^{r,x}$ filter, which has the effect of a single 180° pulse for those protons that are not attached to a ^{13}C nucleus (remotely attached) [26,28]. Other protons (those directly attached to ^{13}C nucleus) are unaffected. If a $[BIRD]^{r,x}$ pulse is applied at the center of an evolution period, the following aspects have to be considered:

1. At the end of the evolution period there will be no effect of the homonuclear J coupling between protons directly attached to ^{13}C and those attached to ^{12}C, since the latter have experienced a 180° pulse.
2. For the same period of time, the heteronuclear $^1J_{HC}$ coupling will be refocused.
3. Notably, the proton chemical shift is not refocused by the $[BIRD]^{r,x}$ filter.
4. Three different spin topologies, ^{13}CH, $^{13}CH_2$ and $^{13}CH_3$, will have to be considered.

These attractive properties have been exploited earlier to design carbon detected HETCOR type 2D experiments, where a $[BIRD]^{r,x}$ building block was inserted into the pulse sequence at the midway of the proton t_1 evolution period. Those spectra displayed cross peaks with no multiplet structure along the proton chemical shift axis and were hence proton–proton J decoupled along the indirect dimension. An isotope selective spin-inversion filter, like the $[BIRD]^{r,x}$ cascade, has the ability to decouple proton spin magnetization even in the case of total spectral overlap, since the selective proton inversion is independent of a given inversion bandwidth.

In this paper, we have used this concept together with our data processing technique to create a new set of HSQC pulse schemes (Fig. 4, pulse sequence B and C). The new technique produces HSQC spectra featuring cross peaks with no multiplet structure for their proton signals. Fig. 4 (Pulse sequence B) demonstrates an experiment based on a pseudo 3D. As displayed a regular echo/antiecho HSQC is prepended to the $[BIRD]^{r,x}$ cascade, which suppresses unwanted ^1H signals attached to ^{12}C atoms. Proton chemical shift evolution is achieved by incrementing the t_1 evolution delay around the $[BIRD]^{r,x}$ building block by the length of a complex dwell time in t_3. In contrast to pulse sequence A (Fig. 1), we have eliminated the constant time evolution period, since there is no necessity to keep the evolution of proton spin relaxation constant too.

The application of the $[BIRD]^{r,x}$ filter on proton spin magnetization has the effect of keeping the evolution of scalar J_{HH} coupling constant, while chemical shift Ω and relaxation R are passing unaffected through the filter. Consequently, there is no J_{HH} modulation

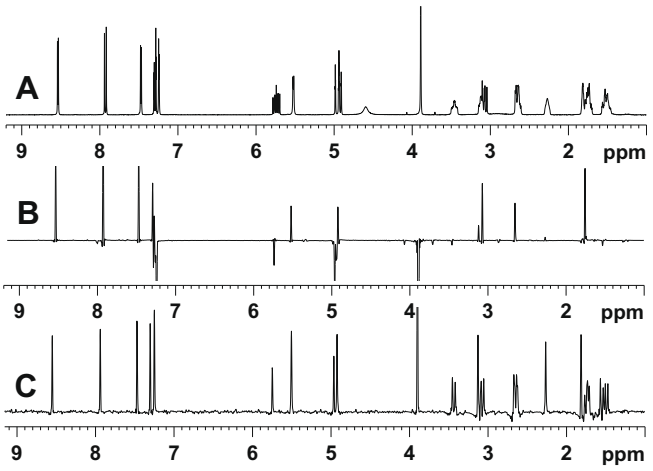

Fig. 3. (A) displays the standard 1D proton spectrum of Quinine in chloroform recorded at 400.13 MHz. (B) represents a pure shift spectrum, acquired by utilizing the pulse sequence A (Fig. 1). The pure shift proton spectrum has an absorptive mode line shape. The spectral bandwidth in observe proton dimension was 10 ppm (4 kHz) leading to an acquisition time of 128 ms in t_2 (512 complex data points in t_2). A constant time period of 128 ms was used for the proton chemical shift evolution in t_1 (512 data points). The relaxation delay was 1 s. The data was processed according to our new strategy discussed in the paper. Up to 64 columns from the 2D data matrix were coadded to produce the final FID. The peak intensities are severely affected by the evolution of homonuclear J coupling and relaxation. (C) shows a pure shift proton spectrum acquired by utilizing pulse program B (Fig. 4). The homonuclear decoupled proton spectrum was derived by processing the t_1/t_3 2D plane of the first ^{13}C evolution increment. The pulse program B (Fig. 4) combines our CT data processing approach with the BIRD pulse selection in a HSQC sequence. The signal amplitudes are represented correctly and the spectrum has an absorptive mode line shape. The effect of relaxation is eliminated, since we use an initial t_1 evolution delay of 3 μs. A detailed description of the method is given in the text. Diastereotopic CH_2 groups show a doublet pattern as an irreducible multiplicity.

caused by t_1 incrementation along ω_1 time axis. Due to the fact, that the t_1 evolution is synchronized with the dwell time in the observe dimension, there will be no truncated relaxation behavior and we obtain a smooth decay by relaxation after FID reconstruction of the decoupled spectra.

The time, in which proton spin magnetization is in the transverse plane, can thus be minimized and as a result of avoiding T2 relaxation the sensitivity of the method is greatly enhanced. Now, for each ^{13}C t_2 evolution increment, a 2D plane along the t_1/t_3 dimension is recorded until the total number of desired data points in t_2 (^{13}C) is acquired. Each such 2D plane was processed according to our processing strategy as described above (Eqs. (1)–(5)) to deliver a FID of a 1D broadband decoupled proton spectrum (Fig. 4). This was then stored in a 2D data matrix. The signal intensities are modulated by the evolution of ^{13}C chemical shift. A 2D FT produces a HSQC spectrum featuring cross peaks with collapsed proton multiplicities.

The features of the J selective spin inversion decoupling technique imply a certain conjunction with the given spin topologies CH, CH_2 and CH_3. Protons existing in a diastereotopic CH_2 spin topology remain unaffected by the effect of the $[BIRD]^{r,x}$ cascade and therefore continue to evolve their geminal spin–spin ($^2J_{HH}$) coupling over the course of the evolution period. We refer to this type of $^2J_{HH}$ spin–spin splitting as irreducible multiplicity. The cross peaks stemming from diastereotopic CH_2 groups show a residual $^2J_{HH}$ doublet splitting, which can not be further reduced.

The 3D data set produced by pulse sequence B (Fig. 4) was stored and processed according to the procedure outlined above to deliver the HSQC spectrum presented in Fig. 5e–h. The collapse of the proton multiplet structures allows an unambiguous and straightforward assignment of cross peaks. The ones belonging to diastereotopic CH_2 protons display a J splitting in the proton chem-

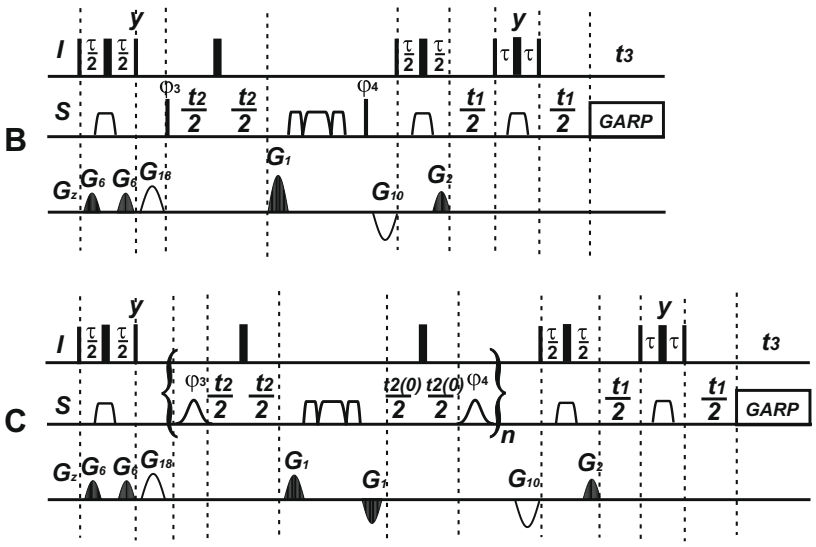

Fig. 4. For obtaining broadband homonuclear decoupled HSQC spectra, the pseudo 3D pulse sequences B and C are introduced. The proton–proton decoupling and proton chemical shift evolution is carried out in the t_1 evolution period by the $[BIRD]^{r,x}$ pulses. In sequence B a regular HSQC pulse sequence is prepended to the $[BIRD]^{r,x}$ pulses, serving as an X-filter for selecting the protons attached to ^{13}C and for the purpose of ^{13}C chemical shift evolution in t_2. For each single t_2 increment a 2D plane along the t_1/t_3 dimension is recorded. Narrow and wide filled rectangles represent non-selective ^1H 90° and 180° pulses respectively. Unless stated otherwise, pulses are applied along the x-axis. The filled sine shaped pulsed field gradient pulses were 1 ms in length. The crusher pulsed field gradients are indicated as open sine envelopes and are 1 ms in length. The pulsed field gradients are applied along the z-axis for selection or artifact suppression followed by a gradient recovery delay of 100 μs. The chirp pulses are defined in files in the Bruker library: Crp60,0.5,20.1 is a smoothed chirp pulse [30] for inversion with a pulse length of 500 μs and is shown as open trapezoids. Crp60comp.4 [31] is a refocusing pulse with a pulse length of 2 ms and is shown as a triple of open trapezoids. The chirp pulses were defined with 1000 points and 4000 points, respectively, a sweep width of 60 kHz and 20% smoothing. The power of the chirp pulse was adjusted to a level equivalent to that of a 90° rectangular pulse of 25.5 μs (9.8 kHz), which corresponds to a Q factor of 5 (determined with ShapeTool). The homonuclear decoupled HSQC spectrum was recorded using 2 scans per increment and 500 ms relaxation delay. The following delay parameter was used: $t = 1/(2J_{CH}) = 3.45$ ms, initial values for t_1 and t_2 increments were 3 μs. Frequency discrimination in the ^{13}C evolution dimension is achieved by an Echo/antiEcho-TPPI protocol. Broadband adiabatic ^{13}C decoupling [32] was applied during the acquisition (t_2) using a 1.5 ms chirp pulse at a field strength ($\gamma B_1 \max/2\pi$ of 1.8 kHz utilizing a decoupling supercycle given in the Bruker library: p5m4sp180. The following phase cycling was used for the pulse sequences: $\varphi_3 = 0\ 2$, $\varphi_4 = 0\ 0\ 2\ 2$, $\varphi_{rec} = 0\ 2\ 2\ 0$. In sequence C the regular HSQC is replaced by a SHARC–HSQC [29]. Several regions of the ^{13}C spectrum are excited consecutively within a single scan (open gaussian shapes), whereby the carrier frequency is always placed in the center of the region. This leads to a spectrum, in which these bandselective HSQCs are superimposed. Due to the reduced sweepwidth in each of these regions the spectrum can be recorded with the same resolution in a shorter time (or with higher resolution in the same time).

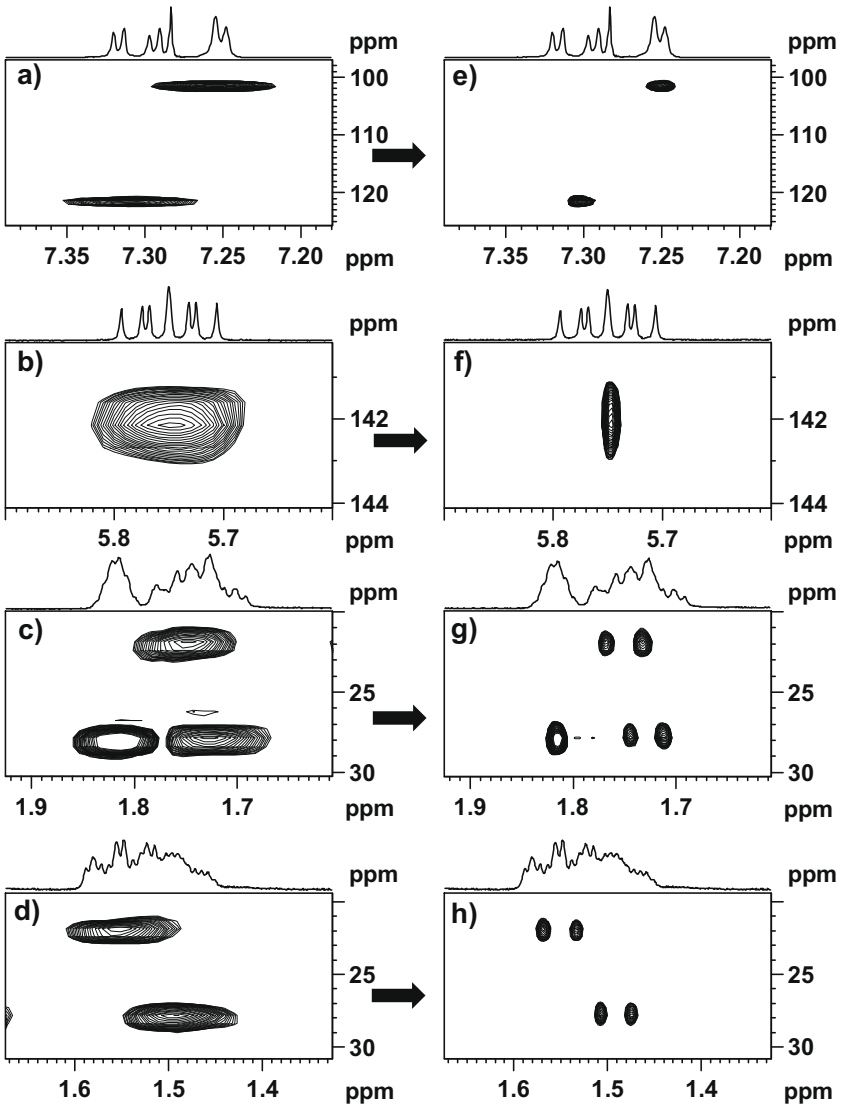

Fig. 5. Regular and homonuclear decoupled HSQC spectra of Quinine in $CDCl_3$ are presented. For a better illustration of the homonuclear decoupling effect on the shape of the proton spin multiplicities, cross peaks from a regular HSQC are displayed in (a–d) (left column). Large proton spin multiplicities are dominating the shape of the cross peaks making an unambiguous assignment difficult. The result of a 2D homonuclear decoupled HSQC spectrum utilizing the pulse sequence B (Fig. 4) is displayed in (e–h) (right column). The spectra clearly demonstrate the effect of homonuclear decoupling on the shape of the cross peaks. Proton spin multiplicities are mostly reduced to singlets and in the case of CH_2 spin systems (diastereotopic protons) an irreducible multiplicity (doublet) is preserved, where the splitting is given by the geminal $^2J_{HH}$ coupling constant. The analysis of the HSQC spectrum becomes much easier. All experiments were acquired on a Bruker-Avance spectrometer (Bruker BioSpin, Rheinstetten, Germany) operating at 400.13 MHz proton frequency, equipped with a double resonance BBO probe and a *z*-axis pulsed field gradient accessory. Spectra were processed with TOPSPIN 2.1. The data were collected on a sample of 90 mM Quinine dissolved in pure chloroform-d_1 at a temperature of 300 K. The sweep width in the observed proton dimension was 10 ppm (4 kHz) leading to an acquisition time of 128 ms in t_3 (512 complex data points). The homonuclear decoupled HSQC spectrum used a sweep width of 140 ppm (t_2(max) of 4.5 ms; 128 data points in t_2) for the ^{13}C evolution dimension and a sweep width of 10 ppm (t_1(max) of 128 ms; 512 data points) for the indirectly detected proton dimension in t_1. The total measurement time was 24 h. A C program was written to process the 3D data set obtained by the pulse program B. The t_1/t_3 2D planes were extracted and each file was processed according to Eqs. (1)–(5) (see text). As a result we obtained 128 1D FIDs of homonuclear decoupled proton spectra, which were put into a 2D HSQC data matrix. The intensities of those signals are modulated by the evolution of the ^{13}C chemical shift. Prior to 2D Fourier transformation, the data were linear predicted by a factor of two in both dimensions, apodized by multiplying with a 90° shifted sine-squared function in both dimensions and then zero-filled to yield final matrices of 256 (^{13}C) × 4K (^1H) real data points.

ical shift dimension. The doublet splitting shown in Fig. 5g–h is the proof for the presence of these geminal $^2J_{HH}$ couplings. Notably, they can be easily extracted from t_2 traces of the HSQC spectrum. We suggest to call those HSQC spectra, where proton multiplicities are mainly collapsed to singlets as RESET HSQC. The acronym RESET stands for Reducing of nuclEar Spin multiplicitiEs to singuleTs.

The sensitivity of the RESET HSQC experiment was determined by comparing its signal-to-noise ratio with corresponding values from a regular HSQC experiment.

A standard HSQC experiment was run under the same experimental conditions as the RESET HSQC to emulate the signal-to-noise behavior of the first HSQC plane (F_2/F_3) out of 512 planes (F_2/F_3). The signal-to-noise ratio of that reference HSQC was determined and multiplied by $(512)^{1/2}$ to give the expectation signal-to-noise ratio of the final spectrum.

According to the signal-to-noise calculation, the RESET HSQC experiment shows a sensitivity, which is 56% of a regular HSQC.

Two sources contribute to the decrease of the sensitivity compared to the reference HSQC spectrum.

The first issue is the contribution of relaxation during the expansion of the t_1 chemical shift evolution period. To investigate these contributions, the signal-to-noise ratio of CH cross peaks from the first and the last (512) F_2/F_3 HSQC planes were analyzed. It turned out that signals from the last HSQC plane (512) possess a residual signal intensity of 60% compared to that from the first HSQC plane. This can be explained by the progress of proton spin

relaxation at the time point t_{1max}, where maximum proton chemical shift evolution is achieved.

The second important issue controlling the final signal-to-noise of the decoupled spectrum is the right choice for the number of complex dwell points to be considered in the t_3 dimension. This was investigated by systematically including up to 256 complex dwell points ($t_{3max} \sim 64$ ms) into our processing scheme and monitoring the change of the signal-to-noise ratio in the resulting spectrum. The maximum contribution to the final signal-to-noise ratio could be achieved by inserting 128 complex dwell points ($t_{3max} \sim 32$ ms) into the processing scheme. Adding more complex dwell points (for example 256, $t_{3max} \sim 64$ ms) will not significantly increase the overall signal-to-noise ratio, but rather the level of artifacts in the decoupled spectrum. The first part is due to the increasing contribution of homonuclear scalar *J* coupling evolution, which will strongly attenuate the signal intensities as t_3 is getting longer. The second aspect can be attributed to the performance of the back-prediction as the number of points to be predicted is getting larger.

The pulse sequence B (Fig. 4) requires quite a large number of data points, 1K (F3) × 128 (F2) × 512 (F1), in order to provide the final spectrum with sufficient digital resolution. In our example, a total measurement time of 24 h was required to record the RESET HSQC spectrum (Fig. 5). This can be reduced by including the idea of Zangger-Sterk. Rather than using 128 complex points to improve the signal-to-noise ratio, some of those can be used to speed up the experiment. Setting the increment (in1) to *n* times the dwell time (dw), the reconstruction would include *n* complex points in t_3 to obtain the new FID, leaving 128/*n* of such blocks to be used for improving the signal-to-noise ratio. With the upper limit of 8 ms for those blocks, a value for n of 32 could be achieved in our case, reducing the experiment time to about 45 min. Thus violating the idea of a constant time experiment and reintroducing *J* evolution into the supposed pure shift dimension has the disadvantage of leading to artifacts in the form of sidebands. Another way to avoid long measurement times is the reduction of the ^{13}C sweep width in the indirect dimension. The measurement time is saved by reducing the number of t_1 increments. Recently, we introduced the SHARC approach, where region selective excitation pulses are used to superimpose reduced spectral bandwidths and hence accelerate HSQC acquisitions [29]. This idea is now combined with the RESET technique to give the pulse sequence C (Fig. 4). Four equal ^{13}C spectral bandwidths of 35 ppm each were recorded using 32 data points in the ^{13}C dimension. With this approach the overall experiment time could thus be reduced to 6 h.

3. Conclusions

In conclusion, the results presented here illustrate that the exclusion of any temporal *J* evolution, either by assuming a constant time period or by using a $[BIRD]^{r,x}$ filter (isotope selection), opens the opportunity to achieve homonuclear chemical shift propagation along an extra dimension. In combination with the described reconstruction scheme this leads to homonuclear broadband decoupled proton spectra. Whereas for proton only experiments spatial and isotope selection show a comparable sensitivity (1–2%), the use of bilinear rotation pulses and delays can be combined with H,C correlation experiments at almost no additional cost. The isotope selective spin inversion filter allows for proton–proton scalar *J* decoupling even in the case of total spectral overlap. A set of HSQC pulse sequences is presented to deliver spectra with collapsed proton spin multiplicities. As a result, broadband proton decoupled proton spectra with absorption mode line shapes in one and two dimensions are routinely accessible. Due to the special spin topology of the diastereotopic CH_2 groups (both protons are attached to ^{13}C via a large $^1J_{HC}$ scalar coupling), an irreducible doublet splitting of cross peaks along the proton chemical shift dimension is retained. The sensitivity of the RESET HSQC was determined to be 56% of that of a regular HSQC.

References

[1] W.P. Aue, J. Karhan, R.R. Ernst, Homonuclear broadband decoupling and two-dimensional J-resolved NMR spectroscopy, J. Chem. Phys. 64 (1976) 4226–4227.
[2] A.J. Shaka, J. Keeler, T. Frenkiel, R. Freeman, An improved sequence for broadband decoupling: WALTZ-16, J. Magn. Reson. 52 (1983) 335–338.
[3] A.J. Shaka, P.B. Barker, R. Freeman, Computer-optimized decoupling scheme for wideband applications and low-level operations, J. Magn. Reson. 64 (1985) 547–552.
[4] P. Jesson, P. Meakin, G.J. Kneissel, Homonuclear decoupling and peak elimination in Fourier transform nuclear magnetic resonance, J. Am. Chem. Soc. 95 (1973) 618–620.
[5] A. Hammarstroem, G. Otting, Improved spectral resolution in ^1H NMR spectroscopy by homonuclear semiselective shaped pulse decoupling during acquisition, J. Am. Chem. Soc. 116 (1994) 8847–8848.
[6] J. Weigelt, A. Hammarstroem, W. Bermel, G. Otting, Removal of Zero-Quantum coherence in protein NMR spectra using SESAM decoupling and suppression of decoupling sidebands, J. Magn. Reson. B110 (1996) 219–224.
[7] E. Kupce, H. Matsuo, G. Wagner, in: Biological Magnetic Resonance, vol. 16, Modern Techniques in protein NMR (Chapter 5), Homonuclear Decoupling in Proteins, 1999, pp. 149–193.
[8] G.A. Morris, R. Freeman, Selective excitation in Fourier transform nuclear magnetic resonance, J. Magn. Reson. 29 (1978) 433–462.
[9] K. Nagayama, P. Bachmann, K. Wuethrich, R.R. Ernst, The use of cross-sections and of projections in two-dimensional NMR spectroscopy, J. Magn. Reson. 31 (1978) 133–148.
[10] J.-M. Nuzillard, Time-reversal of NMR signals by linear prediction. Application to phase-sensitive homonuclear J-resolved spectroscopy, J. Magn. Reson. A 118 (1996) 132–135.
[11] S. Simova, H. Sengstschmid, R. Freeman, Proton chemical-shift spectra, J. Magn. Reson. 124 (1997) 104–121.
[12] G.N. Naganagowda, Spectral simplification and "pseudo decoupling" in one-dimensional proton NMR spectra using pulsed-field gradients, J. Magn. Reson. A 118 (1996) 113–116.
[13] A.J. Pell, R.A.E. Edden, J. Keeler, Broad band proton-decoupled proton spectra, Magn. Reson. Chem. 45 (2007) 296–316.
[14] G.J. Harris, S.R. Lowe, T.J. Norwood, In-phase selective excitation of overlapping multiplets, J. Magn. Reson. 142 (2000) 389–392.
[15] L.D. Hall, T.J. Norwood, A chemical-shift selective filter, J. Magn. Reson. 76 (1988) 548–554.
[16] L.D. Hall, T.J. Norwood, An improved chemical-shift selective filter, J. Magn. Reson. 78 (1988) 582–587.
[17] P.T. Robinson, T.N. Pham, D. Uhrin, In phase selective excitation of overlapping multiplets by gradient-enhanced chemical shift selective filters, J. Magn. Reson. 170 (2004) 97–103.
[18] R. Brüschweiler, C. Griesinger, O.W. Sørensen, R.R. Ernst, Combined use of hard and soft pulses for ^1H decoupling in two-dimensional NMR spectroscopy, J. Magn. Reson. 78 (1988) 178–185.
[19] K. Zangger, H. Sterk, Homonuclear broadband-decoupled NMR spectra, J. Magn. Reson. 124 (1997) 486–489.
[20] P. Giraudeau, S. Akoka, Sources of sensitivity losses in ultra fast 2D NMR, J. Magn. Reson. 192 (2008) 151–158.
[21] A.J. Pell, J. Keeler, Two-dimensional J-spectra with absorption-mode lineshapes, J. Magn. Reson. 189 (2007) 293–299.
[22] M. Nilsson, G.A. Morris, Pure shift proton DOSY: diffusion-ordered ^1H spectra without multiplet structure, Chem. Commun. (2007) 933–935.
[23] J. Santoro, G.C. King, A constant-time 2D overbodenhausen experiment for inverse correlation of isotopically enriched species, J. Magn. Reson. 97 (1992) 202–207.
[24] A. Bax, A.F. Mehlkopf, J. Smidt, Homonuclear broadband-decoupled absorption spectra, with line widths which are independent of the transverse relaxation rate, J. Magn. Reson. 35 (1979) 167–169.
[25] J.R. Garbow, D.P. Weitekamp, A. Pines, Bilinear rotation decoupling of homonuclear scalar interactions, Chem. Phys. Lett. 93 (1982) 504–509.
[26] D. Uhrin, T. Liptaj, K. Koever, Modified BIRD pulses and design of heteronuclear pulse sequences, J. Magn. Reson. A 101 (1993) 41–46.
[27] D. Uhrin, 3D HSQC–HSQMBC – increasing the resolution of long-range proton–carbon correlation experiments, J. Magn. Reson. 159 (2002) 145–150.
[28] A. Bax, Broadband homonuclear decoupling in heteronuclear shift correlation NMR spectroscopy, J. Magn. Reson. 53 (1983) 517–520.
[29] P. Sakhaii, B. Haase, W. Bermel, An alternative approach for recording of multidimensional NMR data based on frequency dependent folding, J. Magn. Reson. 191 (2008) 291–303.
[30] J.M. Boehlen, G. Bodenhausen, Experimental aspects of chirp NMR spectroscopy, J. Magn. Reson. A 102 (1993) 293–301.
[31] T.L. Hwang, P.C.M. van Zijl, M. Garwood, Broadband adiabatic refocusing without phase distortion, J. Magn. Reson. 124 (1997) 250–254.
[32] R. Fu, G. Bodenhausen, Broadband decoupling in NMR with frequency-modulated chirp pulses, Chem. Phys. Lett. 245 (1995) 415–420.